Influence of Water and Filler Content on the Dielectric Response of Silica-Filled Rubber Compounds

ARTICLE *in* MACROMOLECULES · MARCH 2013

Impact Factor: 5.8 · DOI: 10.1021/ma302408z

6 AUTHORS, INCLUDING:

Gustavo Ariel Schwartz
Spanish National Research Council
46 PUBLICATIONS **698** CITATIONS
SEE PROFILE

Silvina Cerveny
Universidad del País Vasco / Euskal Herriko …
55 PUBLICATIONS **1,043** CITATIONS
SEE PROFILE

Juan Colmenero
Universidad del País Vasco / Euskal Herriko …
401 PUBLICATIONS **8,533** CITATIONS
SEE PROFILE

Stephan Westermann
Goodyear
27 PUBLICATIONS **191** CITATIONS
SEE PROFILE

Macromolecules

Article

pubs.acs.org/Macromolecules

Influence of Water and Filler Content on the Dielectric Response of Silica-Filled Rubber Compounds

J. Otegui,[†] G. A. Schwartz,*[,†,‡] S. Cerveny,[†,‡] and J. Colmenero[†,‡,§]

[†]Centro de Física de Materiales (CSIC-UPV/EHU)-Material Physics Centre (MPC), P. M. de Lardizábal 5, 20018, San Sebastián, Spain

[‡]Donostia Internacional Physics Center, Paseo Manuel de Lardizábal 4, 20018, San Sebastián, Spain

[§]Departamento de Física de Materiales, Universidad del País Vasco (UPV/EHU), Facultad de Química, Apartado 1072, 20018, San Sebastián, Spain

J. Loichen and S. Westermann

Goodyear Innovation Center Luxembourg, Global Materials Science, Av. Gordon Smith, L-7750 Colmar-Berg, Luxembourg

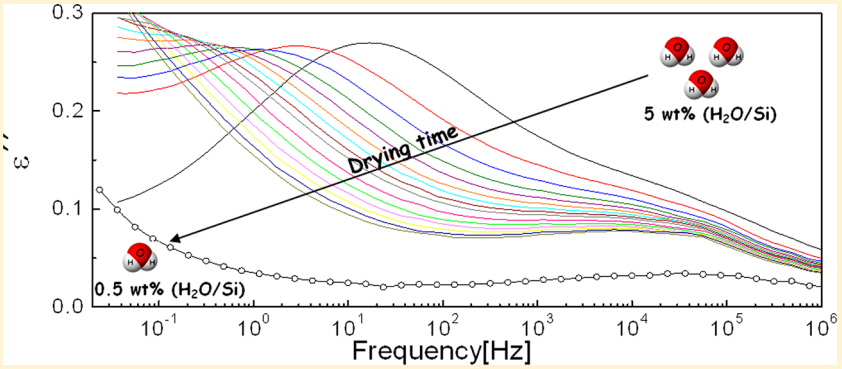

ABSTRACT: We present in this work a systematic study to analyze the influence of water and filler content on the dielectric response of silica-filled rubber compounds. For nanoparticle-filled polymers an additional dielectric process is usually observed in the loss dielectric spectra at frequencies lower than the alpha (α) or segmental relaxation. This process has generated some controversy in the literature due to the different (sometimes contradictory) interpretations given to explain its physical origin. We demonstrate, by means of dielectric spectroscopy in combination with thermal analysis, that this low-frequency process is compatible with a MWS process enhanced by the presence of water molecules at the silica surface. We show that the frequency of the maximum for this process is strongly affected by the amount of water attached to the silica particles. The dielectric response of the MWS process is rationalized by means of a simple interlayer model (IL). In addition, we also study the influence of water and filler content on the segmental dynamics and discuss possible mechanisms for the filler−polymer interaction.

1. INTRODUCTION

Reinforcement of polymers by nanoparticles plays an important role in improving the mechanical properties of polymeric compounds. In particular, styrene−butadiene rubber (SBR) filled with silica particles is widely used in numerous applications—the most important being the tire compounds.[1] This is because silica reduces the rolling resistance leading to lower fuel consumption and provides greater wear resistance and superior wet traction.[2,3] One of the key factors that determine the final properties of the filled compounds is the filler−polymer interaction, which strongly depends on several factors like polymer and filler type, filler surface treatment, chemical additives, and mixing procedure, among others. Several works have been published during the past years concerning the polymer dynamics of unfilled[4−7] and filled rubber compounds[8−11] and especially on the polymer−filler interaction.[12−15] However, despite the big effort done in this area, this interaction is far from being well understood, and contradictory interpretations can be found in the literature.

A powerful tool for investigating the polymer dynamics as well as the polymer−filler interaction in nanoparticles filled compounds is broadband dielectric spectroscopy (BDS).[16] This technique allows measuring the dielectric response over a broad frequency and temperature range, giving valuable information about both the molecular dynamics of the polymer chains and the polymer−filler interface. For unfilled SBR two relaxation processes are usually observed in the dielectric spectra:[7] the α-relaxation, involving cooperative motions, and the secondary

Received: November 21, 2012
Revised: February 11, 2013

   dx.doi.org/10.1021/ma302408z | *Macromolecules* XXXX, XXX, XXX−XXX

(or β-) relaxation, concerning the local motions (in polymers, the β-process can be usually related with the movement of lateral groups). However, when nanoparticles are added to SBR, an additional dielectric process is observed at frequencies lower than the α-relaxation. According to some authors, this process is caused by blocking of charge carriers at internal surfaces of different phases (interfaces) having different values of the dielectric permittivity and/or conductivity.[17,18] It is well-known that heterogeneous systems including interfaces (such as particle suspensions,[19,20] semicrystalline polymers,[21] blends,[22,23] and nanocomposite materials[24−28]) usually show a dielectric process attributed to the Maxwell−Wagner−Sillars (MWS) polarization. This process has been observed for rubber systems filled with carbon black,[29] graphite,[30] and silica.[11,31]

On the other hand, some researchers attribute this process to a second α-relaxation process associated with the polymer fraction attached to the filler particles.[32,33] For polymeric nanocomposites, a significant fraction of the polymer is within a distance of a few nanometers from the particle surface. According to these works, this interfacial polymer should have different structural and dynamics properties. It is argued that this thin layer of interfacial polymer has a restricted mobility due to the strong interaction between filler and polymer, being the origin of this second α-relaxation process.

The main purpose of this work is to establish that the origin of the low-frequency process observed for silica-filled SBR compounds in BDS is the MWS polarization. In addition, we will show that this process is enhanced by the presence of water molecules at the silica surface. The experimental data are well described by a simple model, which considers the water layer around the silica particles dispersed in the SBR matrix. In addition, we will analyze how water molecules affect the dielectric properties of silica SBR nanocomposites by studying the effect of drying and rehydrating. Finally, we will also discuss how the filler and water content affects the α-relaxation process.

2. EXPERIMENTAL SECTION

2.1. Materials. The polymer used in this work was solution styrene−butadiene rubber (S-SBR) BUNA VSL 5025. S-SBR has 25% styrene, 50% 1−2 vinyl, 15.4% 1−4 trans, and 9.6% 1−4 cis comonomer distribution. The filler used was precipitated amorphous silica (Z1165 MP-Rhodia) with a specific surface area of 165.8 m^2/g. Compounds with three different volume fraction of filler (0, 30, and 90 phr, where phr = per hundred rubber (parts in weight per 100 parts of rubber)) were prepared (see Table 1 for the composition of each sample). An internal mixer was used for mixing the rubber, the filler, and the rest of the additives. Once the compounds were mixed, square sheets were obtained by compression-molding vulcanization at 170 °C for 10 min in a mold yielding samples of 15 × 15 cm and thickness of about 0.7 mm. The samples from this batch were called "as-received" (AR) samples. Finally, different drying protocols were applied to the AR samples as explained in the next sections.

Table 1. Composition for Unfilled and Filled Compounds

components	unfilled	30 phr[a]	90 phr[a]
rubber (BUNA VSL 5025_0)	100	100	100
silica filler (Rhodia Z1165MP)		30	90
TESPD (link agent) bis(3-triethoxysilylpropyl) disulfide		2.4	7.2
antioxidant [*N*-(1,3)-dimethylbutyl-*N*′-phenyl-*p*-phenylenediamine]	2.5	2.5	2.5
stearic acid	3	3	3
TDAE oil	15	15	15
zinc oxide	2.5	2.5	2.5
accelerator [*N*-cyclohexyl-2-benzothiazolesulfeneamide]	2.3	2.3	2.3
sulfur	1.5	1.5	1.5
DPG secondary accelerator, diphenylguanidine		1	2

[a]phr = per hundred rubber.

2.2. Vacuum Drying (VD). The "as-received" (AR) samples were dried at 100 °C in a vacuum oven for 3 days. At this temperature most of the water was evaporated.

2.3. Rehydration Process (R). After vacuum drying, the samples were transferred to a hydration chamber where both the relative humidity (RH) and the temperature can be controlled. Rubber compounds were rehydrated by exposing them to different relative humidity levels (from 10RH to 70RH) at a temperature of 22 °C. The samples were maintained at constant relative humidity for 4 days in order to achieve the equilibrium for each hydration level. Once the samples were rehydrated to the desired level, they were immediately measured by BDS and TGA.

2.4. BDS Drying (BDSD). The samples were also dried inside the BDS cryostat (under a nitrogen atmosphere) according to the following procedure: first, we measured the dielectric signal at 295 K in the frequency range from 10^{-2} to 10^6 Hz. After that, the sample was dried by heating it at 100 °C for 40 or 90 min depending on the filler content. The dielectric spectrum was then measured again at 295 K, completing one measurement cycle. This procedure was repeated for 800 and 2130 min for 30 and 90 phr, respectively. At the end of the dielectric measurement, TGA were carried out to obtain the corresponding water content.

2.5. Differential Scanning Calorimetry (DSC). DSC measurements were performed by using a DSC Q2000 from TA Instruments in the standard mode. A cooling−heating cycle between −125 and 50 °C with a rate of 10 °C/min was performed using nitrogen as transfer gas. The annealing time between cooling and heating runs was 5 min. Hermetic aluminum pans were used. The glass transition temperature (T_g) was determined at the inflection point of the endotherm curve.

2.6. Thermogravimetry Analysis (TGA). Thermogravimetry measurements were performed for the three "as-received" SBR compounds (unfilled, 30 phr, and 90 phr) focusing on the water evaporation. The measurements were performed using a TGA-Q500 (TA Instruments). All the measurements were conducted under high-purity nitrogen flow over the temperature range 30−1000 °C with a ramp rate of 5 °C/min. In TGA experiments, the sample weight loss was recorded while the temperature was increased. The weight loss and its derivative with respect to the temperature give us valuable information about decomposition of the different components of the sample. In particular, this method is appropriate to determine the amount of water in the compounds.

2.7. TGA Method Used To Obtain the Water Content. Figure 1 shows typical thermographs for unfilled (a) and silica filled SBR compounds (b). In these curves, up to three different weight drops (or three peaks in the derivative plot) are observed. In the case of unfilled SBR (see Figure 1a) two peaks are visible; one around 200 °C (associated with oil evaporation[34]) and the other one between 300 and 450 °C (due to rubber decomposition[34]). For filled compounds (see Figure 1b), an extra weight loss can be observed at low temperatures. The first rapid initial drop of the mass (from room temperature up to ∼200 °C) corresponds to the loss of water adsorbed on the surface of silica.[35,36] In the weight derivative plot this mass drop is seen as a peak, herein namely "water peak". Defining T_1 as the onset of the oil peak in the weight derivative plot (where most of the water has been evaporated) and using the weight percentage $m(T_1)$, we can obtain an estimation of the water content (c_w) in our compounds. This percentage is about 2 wt % for AR90phr and about 1 wt % for AR30phr (see Table 2). The water content normalized to the silica content in the compounds ($c_w/c_{Si} \times 100$) can be calculated dividing the total water content by the silica content after subtracting the final weight obtained for the unfilled SBR ($m_{1000\ °C}$) related with the nonvolatile components (ZnO) (see last column in Tables 2−4).

2.8. Broadband Dielectric Spectroscopy (BDS). Broadband dielectric spectroscopy (BDS) was performed on disk-shaped samples

dx.doi.org/10.1021/ma302408z | Macromolecules XXXX, XXX, XXX−XXX

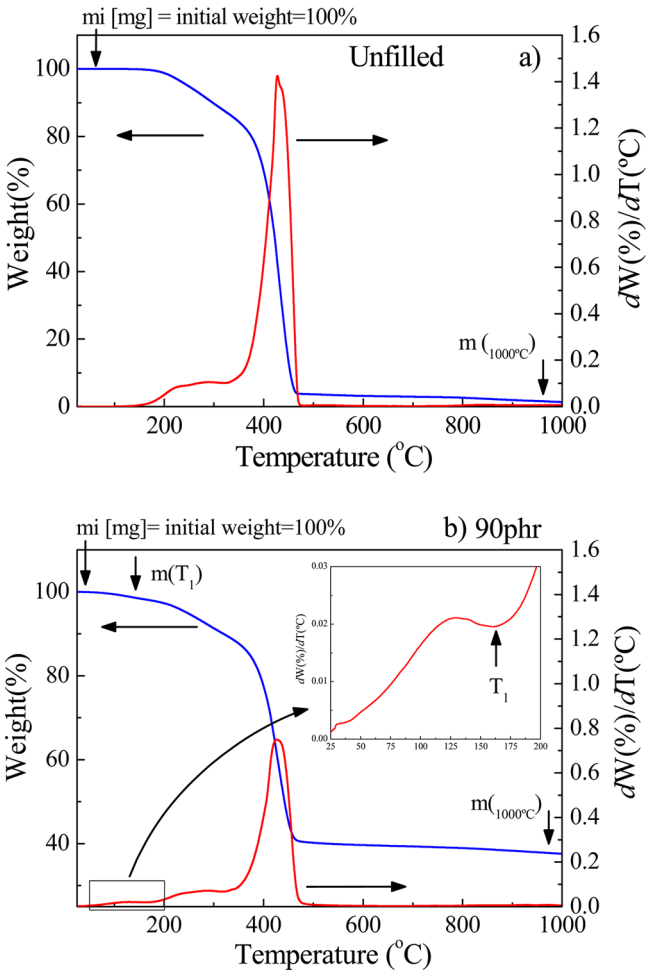

Figure 1. Thermogravimetric measurements (TGA) obtained for the (a) unfilled and (b) filled compounds.

with a diameter of 40 mm (or 20 mm) and a thickness typically of about 0.7 mm. The samples were placed between gold parallel plate electrodes. For parallel-plate configuration, the sample capacitance is expressed as $C = \varepsilon d/A$, where ε is the dielectric permittivity of the sample, A is the section, and d its thickness. The material properties are characterized by the complex dielectric permittivity, ε^*, which is defined as $\varepsilon^*(\omega) = C^*(w)/C_0 = \varepsilon'(\omega) - i\varepsilon''(\omega)$, where C_0 is the capacitance of the free space and $\omega = 2\pi f$. A broadband high-resolution dielectric spectrometer (Novocontrol Alpha) was used to measure the complex dielectric permittivity, $\varepsilon^*(\omega) = \varepsilon'(\omega) - i\varepsilon''(\omega)$, in the frequency range from 10^{-2} to 10^6 Hz. Isothermal frequency scans were performed every third degree in the temperature range 253−353 K. The sample temperature was controlled by a nitrogen gas flow that provides temperature stability better than ±0.1 K.

3. RESULTS

Figure 2 shows the isothermal dielectric loss spectra $\varepsilon''(f)$ at 295 K for "as-received" silica-filled SBR (AR30phr and

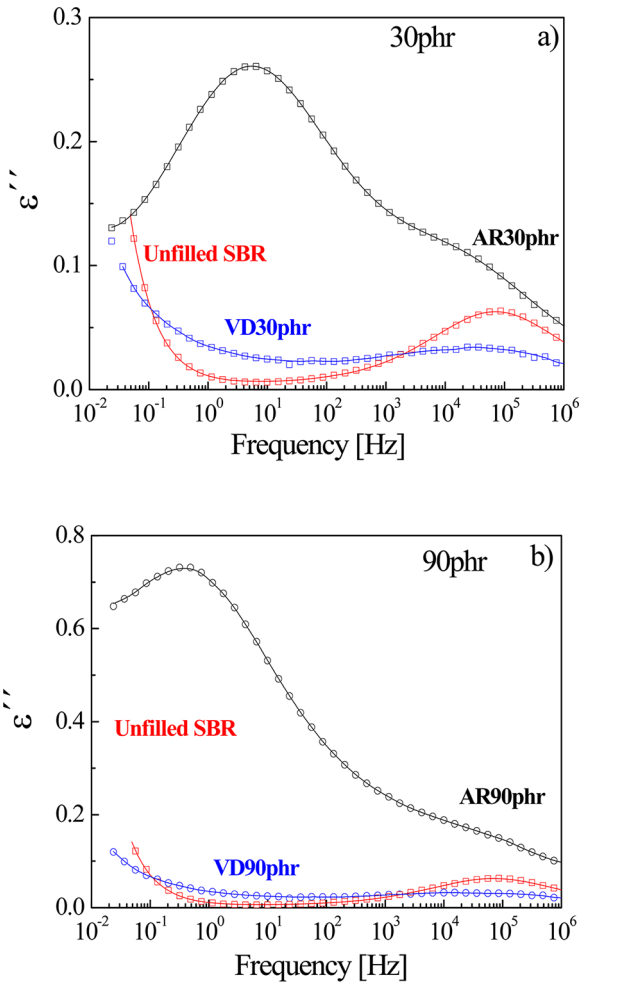

Figure 2. Dielectric loss spectra at a fixed temperature (295 K) for unfilled SBR (red □) and (a) AR30phr (black □) and VD30phr (blue □) and (b) AR90phr (black ○) and VD90phr (blue ○). Solid lines represent the resulting fit function (see text).

AR90phr) and silica-filled SBR after vacuum drying (VD30phr and VD90phr). In addition, the unfilled SBR dielectric spectrum was included in both figures. The spectra of the AR samples (Figure 2a,b) exhibit a well-defined α-relaxation at high frequencies and a strong peak in the dielectric loss at lower frequencies. This process has been attributed to a Maxwell−Wagner−Sillars polarization and was also observed for other rubber compounds.[35,36] Figure 2 also shows how the

Table 2. Initial Sample Weight (m_i), Temperature at Which the Water Content Was Determined (T_1), Weight Percentage at T_1 ($m(T_1)$), Water Content (c_w), Final Weight Percentage at 1000 °C ($m_{1000\ °C}$), Silica Content (c_{Si}), and Water Content Normalized to Silica Content ((c_w/c_{Si}) × 100) for 30 and 90 phr Silica-Filled SBR

samples	m_i [mg]	T_1 [°C]	$m(T_1)$ [wt %]	c_w [wt %]	$m_{1000\ °C}$ [wt %]	c_{Si} [wt %]	$c_w/c_{Si} \times 100$ [wt %]
unfilled	9.869		0.0	0.0	1.361		0.0
AR30phr	13.013	155.12	99.05	0.95	18.3	17.00	5.57
VD30phr	15.557	153.23	99.88	0.12	18.83	17.47	0.69
AR90phr	18.486	165.87	98.09	1.91	37.61	36.30	5.30
VD90phr	13.77	164.74	99.88	0.12	38.32	36.93	0.32

dx.doi.org/10.1021/ma302408z | Macromolecules XXXX, XXX, XXX−XXX

filler content affects both the position and the intensity (dielectric strength) of the MWS process. Moreover the intensity of this process is about 3 times higher for the AR90phr compared to AR30phr; i.e., the MWS relaxation is slower and more intense with increasing silica content.

Surprisingly, for the samples dried in the vacuum oven, the MWS process disappears from the experimental window and only the α-relaxation process remains (besides some conductivity). According to these results, drying of the samples seems to have a strong effect on the MWS process. In the following, we will see that water molecules on the surface of the silica particles strongly affect the behavior of this process.

3.1. Determining the Water Content. TGA measurements were carried out to obtain the water content in the samples before and after drying. Figure 3 shows thermogravimetric weight derivative plots in the water peak region (T < 200 °C) for unfilled SBR, AR silica-filled SBR (AR30phr and AR90phr), and silica-filled SBR after vacuum drying (VD30phr and VD90phr). For AR silica-filled SBR the water peak increases with increasing silica content, suggesting that the total water content increases due to the greater silica surface area where water molecules can link. This is in agreement with the fact that when normalized to the amount of silica, the water content is the same for all AR filled samples regardless of the silica content (see Table 2). On the other hand, the peak related to water molecules moves to higher temperatures with increasing silica content. This temperature increment could be related to the increment of aggregates and/or agglomerates when silica content is increased. Inside agglomerates water molecules could be confined, which in turn could hinder their evaporation (increasing the effective evaporation temperature of water). For vacuum-dried samples, water is almost completely removed from silica surface as observed in Figure 3 (the water content calculated is close to zero (see Table 2)). In this context, it seems that the MWS process is in some way related with the presence of water on the silica surface. To further analyze this hypothesis, we perform two different experiments. On the one hand, we dried the samples inside the broadband dielectric spectrometer under a nitrogen flow at 100 °C, and on the other hand, we rehydrated the samples to analyze whether the presence of this process is reversible or not.

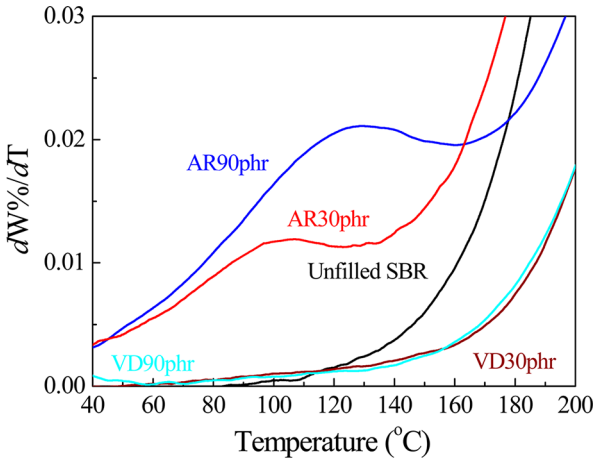

Figure 3. Thermogravimetric weight derivative plot from room temperature up to 200 °C for unfilled SBR, AR30phr, VD30phr, AR90phr, and VD90phr.

3.2. Dielectric Behavior during Drying. The isothermal dielectric loss spectra for AR30 and AR90phr were measured at T = 295 K, at different drying times, following the BDS drying procedure described in section 2.4. Figure 4a,b shows the dielectric loss at different drying times for silica-filled SBR as well as the response for unfilled SBR and vacuum-dried samples. We can clearly see in Figure 4 that by increasing the drying time, the MWS process moves to lower frequencies until leaving the experimental window.

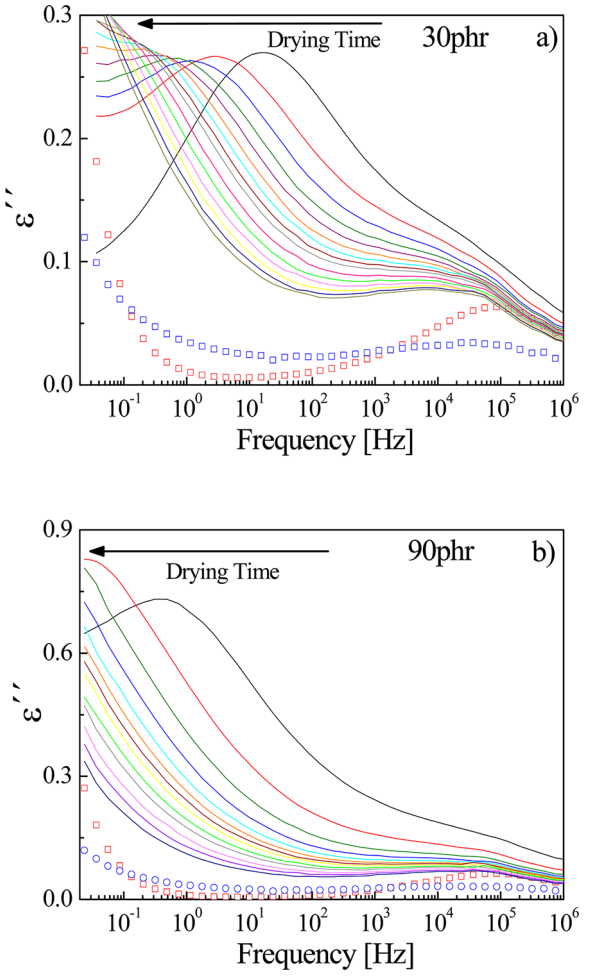

Figure 4. Dielectric loss spectra at fixed temperature (295 K) for (a) BDSD 30phr and (b) BDSD 90phr at different drying times (from 0 to 800 min for the 30phr SBR sample and from 0 to 2130 min for the 90phr SBR sample). Unfilled SBR (red □) and the corresponding samples dried under vacuum at 100 °C for 3 days are also included (VD30phr (blue □), VD90phr (blue ○)).

However, the broadness and the intensity of the MWS peak remain almost constant all along the drying time. After drying the samples in the BDS equipment, the water content was obtained by TGA to confirm that the displacement of the MWS process was related to the water loss in the samples. The water content ($c_w/c_{Si} \times 100$) after the BDS drying procedure was 2.4% for the 30 phr SBR and 3% for the 90 phr SBR: half of the amount obtained for the AR samples. On the basis of these results, we conclude that the shift to lower frequencies observed for the MWS process is related to the amount of lost water. From this experiment we can observe that the vacuum drying does not remove the MWS process but shifts it to lower frequencies until eventually leaves the experimental frequency

dx.doi.org/10.1021/ma302408z | Macromolecules XXXX, XXX, XXX–XXX

window. It is worth to mention here that the α-relaxation is only slightly affected by the drying process.

3.3. Rehydration of Samples. In order to check whether the effect of water on the MWS process is reversible, we rehydrated the dried samples according to the procedure described above section (2.3). Figure 5 shows thermogravimetric weight derivative plots in the water peak region for AR30phr, VD30phr, rehydrated 30 phr silica-filled SBR at 10, 20, 30, 50, and 70 RH and the corresponding samples for 90 phr.

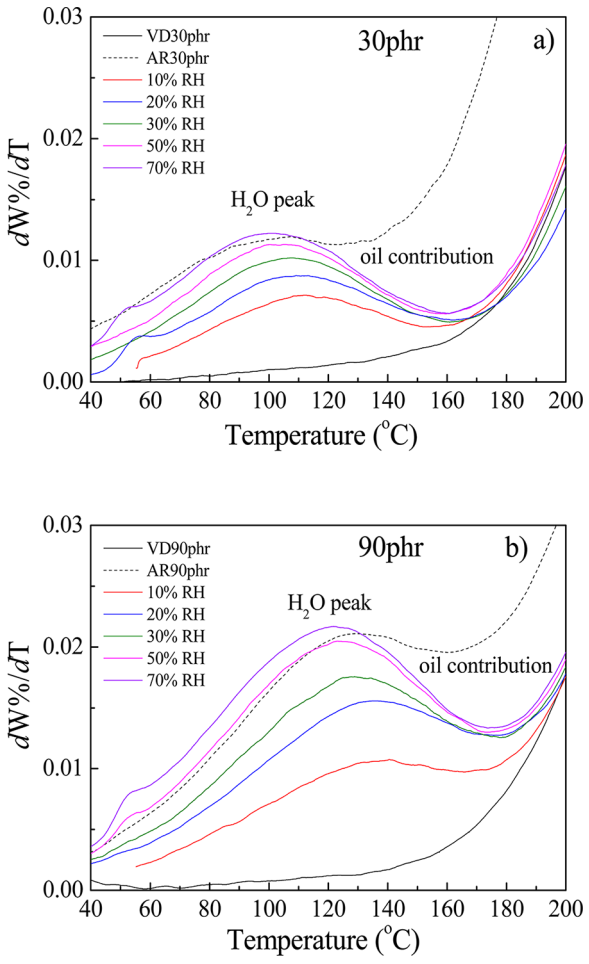

Figure 5. Thermogravimetric weight derivative plot obtained for (a) 30 phr silica-filled SBR and (b) 90 phr silica-filled SBR from room temperature up to 200 °C. From top to bottom: 70% RH, 50% RH, 30% RH, 20% RH, 10% RH, and dried 3 days at 100 °C. Dashed lines represent AR samples.

We observe that the water peak reappears after rehydrating the sample, indicating the reversibility of this process. Moreover, the water peak moves to lower temperatures with increasing water content. This could be explained by the fact that water molecules at the beginning of the hydration are bonded to hydroxyl groups of the silica surface. The next water molecules will be attached to other water molecules and would therefore be easier to remove.[35,36] In addition, Figure 5 shows that the contribution of the oil to the water peak observed between 150 and 200 °C for AR compounds decreases (or is removed) when the samples are dried and rehydrated. This means that some oil molecules (with low evaporation temperatures) are removed together with water molecules during the drying process. This reduction of oil could slightly affect the dynamics of the α-relaxation, making it slightly slower as mentioned in the previous section.

Figure 6 shows the isothermal dielectric loss spectra for the rehydrated compounds. We observe that the MWS process

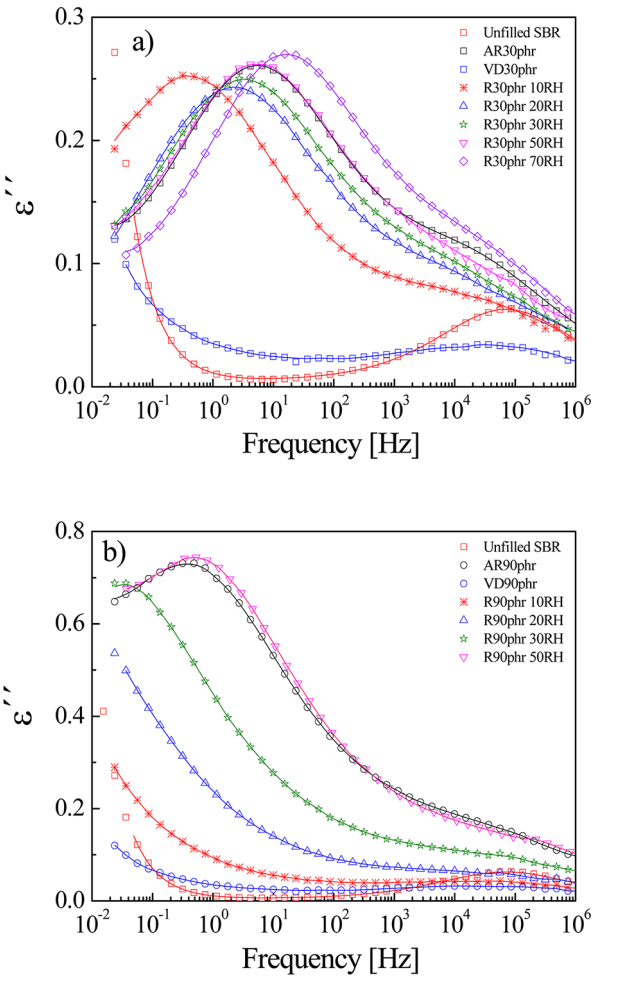

Figure 6. (a) Dielectric loss spectra at fixed temperature (295 K) for AR30phr (black □), VD30phr (blue □), R30phr 10% RH (red ∗), 20% RH (blue △), 30% RH (green ★), 50% RH (red ▽), 70% RH (purple ◇), and unfilled SBR (red □). (b) Dielectric loss spectra at fixed temperature (295 K) for AR90phr (black ○), VD90phr (blue ○), R90phr at 10% RH (red ∗), 20% RH (blue △), 30% RH (green ★), 50% RH (red ▽), and unfilled SBR (red □). Solid lines represent the resulting fit functions.

reappears into the experimental frequency window with increasing water content. For constant filler content, the MWS process moves to lower frequencies by drying the samples and moves back to higher frequencies when the samples are rehydrated. Tables 3 and 4 show the water content normalized to the silica content ($c_w/c_{Si} \times 100$) for these samples. The water content for AR30phr sample is the same than for rehydrated 30phr 50RH sample (5.5 wt %), and Figure 6a shows that the relaxation time of both samples also agree. For higher water contents, the relaxation time of the MWS process becomes even faster than for the AR sample. For 90phr silica filled compound a similar behavior is observed.

3.4. Fitting the Dielectric Spectra. Figure 7 shows the dielectric loss spectra obtained at some selected temperatures for the SBR compounds filled with 90 phr of silica. As we have

dx.doi.org/10.1021/ma302408z | Macromolecules XXXX, XXX, XXX−XXX

Table 3. Relative Humidity (RH), Initial Sample Weight (m_i), Temperature at Which the Water Content Was Determined (T_1), Weight Percentage at T_1 ($m(T_1)$), Water Content (c_w), Final Weight Percentage at 1000 °C ($m_{1000\ °C}$), Silica Content (c_{Si}), and Water Content Normalized to Silica Content ($(c_w/c_{Si}) \times 100$) for 30 phr Silica-Filled SBR

RH	m_i [mg]	T_1 [°C]	$m(T_1)$ [wt %]	c_w [wt %]	$m_{1000\ °C}$ [wt %]	c_{Si} [wt %]	$c_w/c_{Si} \times 100$ [wt %]
as-received (AR)	13.013	155.12	99.05	0.95	18.3	17.00	5.57
vacuum dried (VD)	15.557	153.23	99.88	0.12	18.83	17.47	0.69
10	13.427	154.55	99.45	0.55	18.41	17.05	3.23
20	14.243	159.02	99.25	0.75	18.53	17.17	4.37
30	16.885	164.70	99.14	0.86	18.66	17.30	4.97
50	20.137	162.87	99.04	0.96	18.64	17.28	5.55
70	13.945	166.99	98.89	1.11	18.40	17.04	6.51

Table 4. Relative Humidity (RH), Initial Sample Weight (m_i), Temperature at Which the Water Content Was Determined (T_1), Weight Percentage at T_1 ($m(T_1)$), Water Content (c_w), Final Weight Percentage at 1000 °C ($m_{1000\ °C}$), Silica Content (c_{Si}), and Water Content Normalized to Silica Content ($(c_w/c_{Si}) \times 100$) for 90 phr Silica-Filled SBR

RH	m_i [mg]	T_1 [°C]	$m(T_1)$ [wt %]	c_w [wt %]	$m_{1000\ °C}$ [wt %]	c_{Si} [wt %]	$c_w/c_{Si} \times 100$ [wt %]
as-received (AR)	18.486	165.87	98.09	1.91	37.61	36.30	5.30
vacuum dried (VD)	13.77	164.74	99.88	0.12	38.32	36.93	0.32
10	15.635	168.85	99.08	0.92	38.33	36.97	2.49
20	15.436	180.04	98.54	1.46	37.89	36.53	4.00
30	12.486	181.84	98.32	1.68	38.02	36.66	4.58
50	11.668	182.04	97.99	2.01	37.79	36.43	5.52
70	14.750	182.77	97.81	2.19	37.43	36.07	6.07

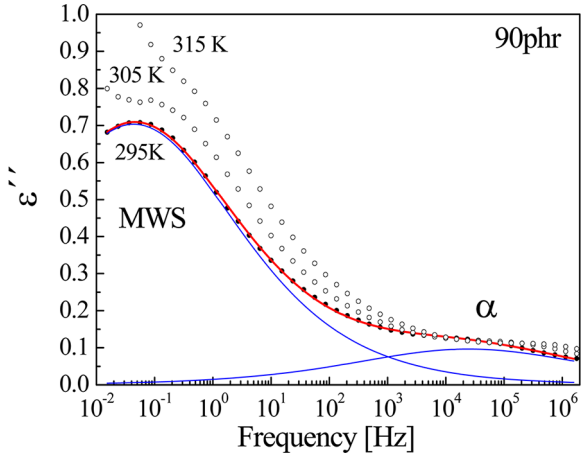

Figure 7. Imaginary part of the dielectric permittivity against the frequency for 90 phr filled SBR at 295, 305, and 315 K and the corresponding fitting functions at 295 K. Solid lines represent the resulting total (red line) and component (blue line) fitting functions.

already mentioned, two different processes are observed: a high-frequency relaxation process associated with the α-relaxation of the polymer and a low-frequency process associated with the MWS polarization.

For the analysis of the dielectric spectra we have used the Cole–Cole function (CC):[41]

$$\varepsilon^*(\omega) = \varepsilon_\infty + \frac{\Delta\varepsilon}{1 + (i\omega\tau)^\alpha} \quad (1)$$

where $\Delta\varepsilon$ is the relaxation strength, τ is the relaxation time, ω is the angular frequency, and α is a shape parameter ($0 < \alpha \leq 1$). The dielectric loss, $\varepsilon''(f)$, for all the samples was described by using two CC functions to take into account the MWS process and the α-relaxation. At high temperatures/low frequencies a conductivity term ($\sigma/(i\varepsilon\omega_0)$) was also included. An example of the resulting fitting is shown in Figure 7.

Figure 8 shows the temperature dependence of the relaxation times corresponding to the MWS process and α-relaxation for as-received and rehydrated samples at two different filler contents: 30 phr (a) and 90 phr (b). A direct inspection of this figure shows that the α-relaxation is hardly affected by both the filler and water content. The temperature dependence of τ_α can be well described by the Vogel–Fulcher–Tammann (VFT) equation[42]

$$\tau(T) = \tau_0 \exp\left(\frac{DT_0}{T - T_0}\right) \quad (2)$$

where τ_0 is the high-temperature limit of the relaxation time and T_0 the temperature at which it diverges. Extrapolation of this formula to a relaxation time of τ = 100 s gives a dielectric estimation of the glass transition temperature, $T_{g,100s}$. This value and the VFT parameters describing the temperature dependence of the α-relaxation time are given in Table 5 for all the samples.

In contrast to the α-process, the relaxation times corresponding to the MWS process are highly dependent on both filler and water content. Its temperature dependence can be described by an Arrhenius equation, $\tau = \tau_0 \exp(E_a/(kT))$, where E_a represents the activation energy and k is the Boltzmann constant. As observed in Figure 8, E_a values depend on filler content but not significantly on water content. The activation energy E_a was calculated, and the average values are 51.9 ± 3.4 and 42 ± 2.2 kJ/mol for 30 and 90 phr, respectively. The higher activation energy values observed for low filler contents can be rationalized if we consider that the mean distance between filler aggregates increases with decreasing filler contents.[27]

4. DISCUSSION

In the previous section, we have shown that for AR silica-filled SBR a MWS process is observed at frequencies lower than the α-relaxation. After drying, this process is no longer detected within our experimental frequency window, as shown in Figure

dx.doi.org/10.1021/ma302408z | Macromolecules XXXX, XXX, XXX–XXX

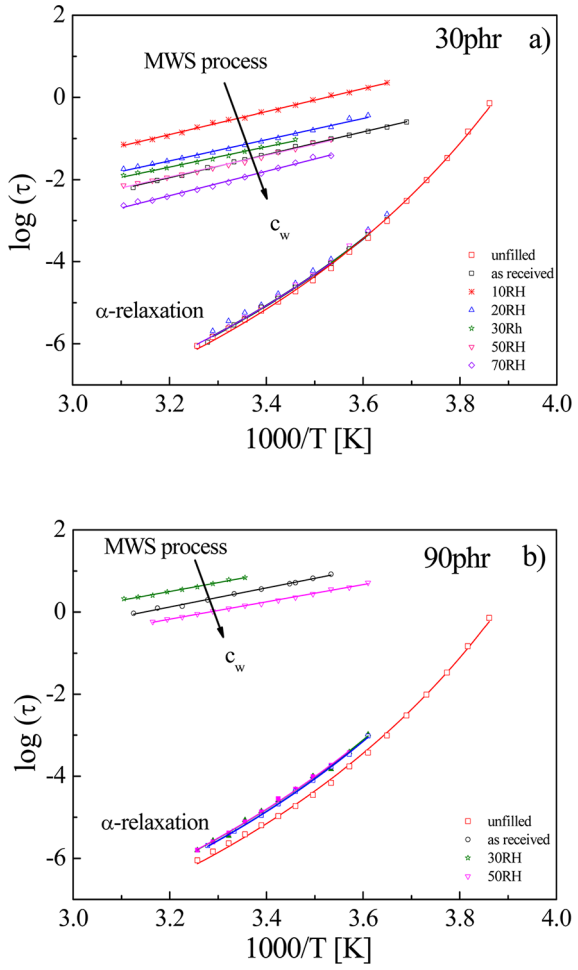

Figure 8. Temperature dependence of the relaxation times for the MWS and α-relaxation processes at different water contents. Unfilled SBR (red □), AR30phr (black □), AR90phr (black ○), 10% (red ∗), 20% (blue △), 30% (green ★), 50% (red ▽), and 70% (blue ◇) relative humidity (RH). The solid lines are the fittings of the experimental data by means of the Arrhenius equation for the MWS process and the VFT equation for the α-relaxation.

Table 5. Fitting Parameters of the VFT Equation for the α-Relaxation of Unfilled and 30 and 90 phr Filled Compounds[a]

	D	T_0 [K]	log(τ_0) [s]	$T_{g,100s}$ [K]
unfilled	7.5 ± 0.1	205.2 ± 0.8	12.8 ± 0.5	250.4 ± 1.4
		30 phr		
AR30phr	8.1 ± 0.1	202.0 ± 0.5	−12.8 ± 0.5	250.6 ± 1.1
10	8.2 ± 0.2	200.5 ± 1.6	−12.8 ± 0.5	248.8 ± 2.3
20	8.2 ± 0.1	201.1 ± 1.4	−12.8 ± 0.5	249.5 ± 2.0
30	8.3 ± 0.1	200.5 ± 1.1	−12.8 ± 0.5	249.3 ± 1.7
50	8.4 ± 0.1	200.2 ± 1.0	−12.8 ± 0.5	249.5 ± 1.6
70	8.3 ± 0.2	200.6 ± 1.4	−12.8 ± 0.5	249.4 ± 2.1
		90 phr		
AR90phr	8.3 ± 0.1	202.2 ± 0.4	−12.8 ± 0.5	251.5 ± 1.0
30	8.5 ± 0.2	200.8 ± 1.8	−12.8 ± 0.5	250.9 ± 1.0
50	8.5 ± 0.2	200.9 ± 1.4	−12.8 ± 0.5	251.1 ± 1.0

[a] T_{g100s} indicates the extrapolation of the relaxation time to 100 s.

2. In addition, we also verified by TGA that in the dried samples no mass loss between 100 and 150 °C is observed. All these results indicate that some volatile component is being removed during the drying process. According to previous works,[39] we assumed that most likely water molecules bounded to silica surface are removed during the drying process. To confirm this hypothesis, we rehydrated the dried samples and we verified that (1) the MWS process reappears into the experimental frequency window (see Figure 6) and (2) the TGA curves show again the corresponding loss mass peaks at the same temperatures (Figure 5). It is worth to remark that in the case of the unfilled sample TGA experiments do not show any loss mass peak between 100 and 150 °C, which clearly indicates that the presence of water molecules is related with the silica particles. Furthermore, by drying the sample within the dielectric cell, we can observe how the MWS polarization gradually moves to lower frequencies with increasing drying time (Figure 4), indicating that the frequency of the maximum of the peak depends on the water content. All this experimental evidence suggests that the MWS process is mainly driven by the water at the surface of the silica particles. In the following we will analyze how water and filler content affect the dielectric response of silica filled SBR compounds.

4.1. Water-Enhanced MWS Process. It is well-known that the dynamics of heterogeneous systems can lead polarization effects due to the difference in the dielectric properties of the components. In particular, the MWS polarization process has been observed in inhomogeneous materials such as semicrystalline polymers,[18] polymeric blends,[20,21] and nanocomposites.[23] In particular, Banghegyi and Karasz[44] observed a low-frequency process in $CaCO_3$-filled polyethylene due to absorbed water, and Woo and Piggot[45] also reported that the presence of a MWS process in glass−epoxy composites is associated with absorbed water.

Different models to calculate the dielectric properties of heterogeneous materials have been developed taking into account the dielectric characteristics of the components.[46−50] In the case of filled polymers, the shape of the fillers, the dielectric properties of both the matrix and filler, and the filler volume fraction have to be taken into account in order to properly describe the dielectric response of the MWS process. In particular, Steeman and co-workers[51] predicted the dielectric response of glass-bead-filled polyethylene having adsorbed water around the particles by using the interlayer model (IL).[49] This model describes the dielectric properties of a three-phase material, which consists of a matrix filled with spherical particles covered by an interfacial layer. The dielectric response of this composite can be calculated if the dielectric properties of the constituents are known. In the IL model, the dielectric properties are derived as a function of the volume fractions (φ_m, φ_p, φ_l) and static dielectric constant (ε_m, ε_p, ε_l) of the three components (m = matrix, p = particle, and l = interlayer).

The main assumptions of the model are (1) the conductivity of the interlayer is independent of the frequency, (2) the filler, the interlayer, and the matrix have a frequency-independent dielectric constant, (3) the volume fraction of the interfacial layer is much smaller than the volume fraction of the filler ($\varphi_l \ll \varphi_p$), and (4) the absolute dielectric constant of the layer is much smaller than the conductivity of the layer divided by the angular frequency ($\varepsilon_l \ll \sigma_l/(\varepsilon_0\omega)$). If these requirements are satisfied, the generalized form of the complex dielectric response (ε_c^*) predicted by the IL model is given by

$$\varepsilon_c^*(\omega) = \varepsilon_\infty + \frac{\varepsilon_s - \varepsilon_\infty}{1 + (i\omega\tau)^\alpha} \quad (\alpha = 1,\ \text{Debye}) \tag{3}$$

dx.doi.org/10.1021/ma302408z | Macromolecules XXXX, XXX, XXX−XXX

$$\varepsilon_s = \varepsilon_m\left(\frac{1+2\phi_p}{1-\phi_p}\right) \quad (4)$$

$$\varepsilon_\infty = \varepsilon_m\frac{(\varepsilon_p+2\varepsilon_m)+2(\varepsilon_p-\varepsilon_m)\phi_p}{(\varepsilon_p+2\varepsilon_m)-(\varepsilon_p-\varepsilon_m)\phi_p} \quad (5)$$

$$\tau = \frac{\phi_p}{1-\phi_p}\frac{3\varepsilon_o}{2\sigma_l\phi_l}[(\varepsilon_p+2\varepsilon_m)-(\varepsilon_p-\varepsilon_m)\phi_p] \quad (6)$$

Our composites can be considered as a three-component system where the silica particles embedded in the SBR rubber matrix are surrounded by an interfacial layer of water. All the assumptions described above are fulfilled for our system, and therefore the IL model can be applied to predict the MWS process. However, our loss peak is much broader than a Debye-type peak. This is because in our compounds we have aggregates and agglomerates that give a distribution of size and distances among them. Thus, we replaced the Debye function in the IL model (which assumes well-dispersed spherical particles of the same size) by the Cole−Cole function in order to take into account the size distribution of the particles and aggregates.

The Cole−Cole shape parameter in eq 3 was taken from the experimental fitting of the corresponding loss spectra ($\alpha = 0.4$). The dielectric constant for the polymer matrix was determined from the low-frequency limit of the real part of the dielectric permittivity of the unfilled SBR sample ($\varepsilon_m = 3.4$). The dielectric permittivity of the silica particles ($\varepsilon_p = 1.8$) was taken from the literature.[52] The value of φ_l was calculated from the water content obtained by TGA considering the volume fraction in Table 1, and σ_l was left as a fitting parameter.

Figure 9 shows the experimental dielectric loss spectra for different samples, after subtracting the α-relaxation and conductivity contributions. In the same figure we show the description (solid lines) obtained by the IL model using the parameters as described in the previous paragraph and leaving σ_l as the only fitting parameter. We can observe an excellent agreement for the position of the dielectric loss peaks at different hydration levels. The inset in Figure 9 shows the so-obtained values for the conductivity of the water layer (σ_l) as a function of water content. We observe that σ_l has an exponential dependence with water content according to previous findings in other systems.[51] Concerning to the intensity of the dielectric response, the model does not precisely account for the dielectric strength observed in the experimental data. Slightly higher values are observed for the experimental dielectric response compared to those predicted by the IL model. We have to take into account that this model assumes spherical particles with homogeneous surface. However, it is well-known that silica particles have a porous and irregular surface[40] that gives more available silica surface (compared to spherical particles), and therefore a larger interlayer area is present in these compounds. The presence of the aggregates and their distribution could also have an influence on the intensity differences observed between the model and the experimental data. All these results allow us to conclude that the low-frequency process observed for these silica-filled SBR compounds is a MWS polarization process due to the different dielectric permittivity between filler and polymer, enhanced by the presence of water molecules around the silica particles.

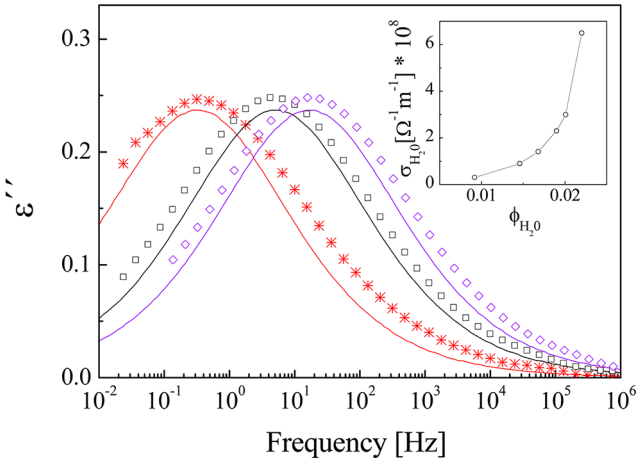

Figure 9. Dielectric loss spectra at fixed temperature (295 K) for R30phr 10% RH (red ∗), AR30phr (black □), and R30phr 70% RH (purple ◇) samples, after subtracting the α-relaxation and conductivity contributions. Solid lines represent the interlayer model (IL) descriptions. Inset: interlayer conductivity σ_l as a function of water volume fraction φ_l.

4.2. Interfacial Polymer around Silica Particles. As already mentioned, it has been argued[32] that the process observed at frequencies lower than the α-relaxation is due to the reduced mobility of SBR at the interface, i.e., polymer segments which are adsorbed at the surface of the nanofillers. Moreover, an effective dielectric glass transition temperature associated with this slow dielectric process (more than 65 °C higher than the bulk glass transition temperature) has been reported.[32] In principle, two glass transitions should be observed by DSC as two separated steps or at least as a very broad single step. However, these features were not observed by us (see Figure 10). Instead, a single glass transition at about

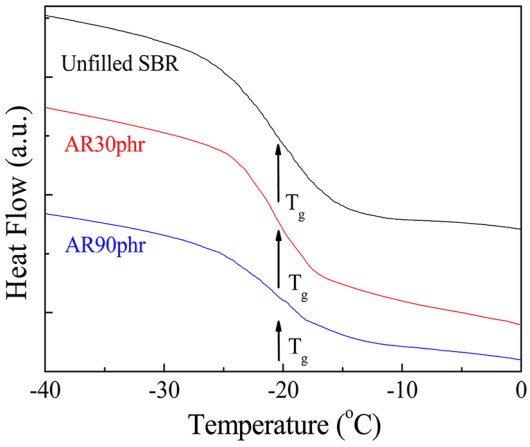

Figure 10. Heat flow as a function of the temperature as obtained from standard calorimetric measurements for unfilled SBR, AR30phr, and AR90phr samples.

252 K is seen for unfilled ($T_g = 252.6 \pm 0.2$ K) and AR silica filled SBR ($T_g = 252.4 \pm 0.3$ K for 30 phr and $T_g = 252.4 \pm 0.4$ K for 90 phr). It is also interesting to note that in these samples the silica nanoparticles do not affect the calorimetric glass transition temperature within the experimental error.

dx.doi.org/10.1021/ma302408z | Macromolecules XXXX, XXX, XXX−XXX

The process observed by Vo et al.[32] is similar to the low-frequency process observed by us in this work. However, we demonstrate in the previous section that this process is a MWS polarization enhanced by water molecules around silica particles. This fact does not mean there are no polymer chains interacting with the filler surface. However, from our results it is clear that the low-frequency process is not reflecting such behavior.

4.3. α-Relaxation. We will now turn to the effect of both water and filler content on the segmental dynamics of the SBR compounds. Following Figure 8, we can observe that the relaxation time is almost independent of water content and slightly depends (for 90 phr) on filler content. It has been observed for some aqueous polymeric solution that water acts as plasticizer increasing the mobility of the polymer and therefore decreasing the glass transition temperature. However, for the compounds here studied, we do not observe any shift in the calorimetric T_g or in the relaxation time. Thus, the segmental relaxation is almost unaffected by the water molecules. From this observation we can assume that, despite of the fact that the structure of our composite is rather complex, the absorbed water is only present at the filler−matrix interface, and therefore no plasticization of the matrix is produced. The absence of water molecules in the polymer matrix is also supported by the TGA measurements that show no water peak for unfilled samples.

The segmental dynamics of the polymeric matrix seems to be slightly (or even not) affected by the presence of the filler, in agreement with previous observations reported for SBR silica nanoparticle compounds[50] and also for other composites.[51−54] At 30 phr the difference is negligible, whereas for 90 phr a small difference is observed between unfilled and filled compounds. However, the dielectric T_g ($T_{g,100s}$) is not affected, and it is the same for all the compounds within the experimental error.

4.4. Polymer−Filler Interaction. Finally, we will focus on the polymer−filler interactions which in a coarse scheme can be divided into two groups: (1) chain segments directly bonded to the filler surface (e.g., chemisorbed) and (2) polymer−filler interaction mediated by coupling agents (e.g., bis(3-triethoxysilylpropyl) disulfide). The samples analyzed here correspond to the second case, where the coupling agent links filler particles to polymer chains through sulfur covalent bounds. This provides a relative flexible link between the polymer chains and the particles surface, and the overall effect is a slight increment of the effective cross-link density. This kind of interaction only slightly affects the α-relaxation of the polymer. In the case of chain segments directly bonded to the filler, the individual monomers are certainly immobilized at the surface, and therefore this kind of link is less flexible than the previous one. However, according to Robertson and Roland,[15] a large fraction of directly bonded segments are necessary to obtain an immobilized phase. This is because the segmental dynamics underlying the glass transition involves conformational transitions of only a few polymeric units. According to the Adam−Gibbs framework,[54] a cooperative rearrangement region (CRR) can be defined with a size related with the relevant length scale where the α-relaxation takes place. The size of the CRR has not been determined for SBR, but on the basis of measurements performed on similar polymers by means of mechanical,[52,53] dielectric,[54,55] and calorimetric methods,[56,57] we can estimate its value between 1 and 2 nm. This means that whatever is the kind of the polymer−filler interaction, it should not affect the segmental dynamics beyond 1 or 2 nm away from the link. Therefore, although there are some published works that seem to unambiguously show the presence of immobilized polymer segments at the surface of the filler particles, it is still not clear whether this polymer−filler interaction will significantly affect the segmental dynamics. We are currently running some experiments to study in depth the α-relaxation of the polymer close and far from the silica surface. These results will be published in a future work.

5. CONCLUSIONS

In this work we have studied the dielectric response of silica-filled SBR compounds. Two processes were observed in the dielectric spectra for the temperature and frequency range here analyzed. The faster process is associated with the segmental relaxation, whereas the slower one is related to the MWS polarization. It was found that the MWS process is directly related with the water layer around the silica particles. The amount of hydration water determines the position of the maximum in the loss spectrum. For high water contents, the MWS peak moves to higher frequencies, whereas for low water contents the peak shifts to lower frequencies. The MWS process can be completely removed from our experimental frequency window for extremely low water contents. This behavior has been rationalized by means of the IL model. With regards to the α-relaxation it was found that the position of the calorimetric glass transition is not affected by the addition of the filler or by the water content. Finally, we have also discussed possible mechanisms for the filler−polymer interaction and its influence on the polymer dynamics.

AUTHOR INFORMATION

Corresponding Author

*E-mail: schwartz@ehu.es.

Notes

The authors declare no competing financial interest.

ACKNOWLEDGMENTS

The authors gratefully acknowledge the support of the Spanish Ministry of Education (MAT2012-31088) and the Basque Government (IT-436-07). The continuous outstanding collaboration and support by Dr. F. Petry and Dr. R. Mruk (Goodyear Innovation Center Luxembourg) are also greatly acknowledged. We also thank the Goodyear Tire and Rubber Company for the permission to publish this paper.

REFERENCES

(1) Bergna, H. E.; Roberts, W. O. *Colloidal Silica: Fundamental and Applications*; CRC Press: Boca Raton, FL, 2006.
(2) Wolff, S.; Wang, M. J. *Rubber Chem. Technol.* **1992**, *65*, 329.
(3) Wang, M. J.; Wolff, S.; Tan, E. H. *Rubber Chem. Technol.* **1993**, *66*, 178.
(4) Klüppel, M.; Heinrich, G. *Macromolecules* **1994**, *27*, 3596.
(5) Klüppel, M. *Macromolecules* **1994**, *27*, 7179.
(6) Marzocca, A. J.; Cerveny, S.; Mendez, J. M. *Polym. Int.* **2000**, *49*, 216. Cerveny, S.; Ghilarducci, A.; Salva, H.; Marzocca, A. J. *Polymer* **2000**, *41*, 2227.
(7) Cerveny, S.; Bergman, R.; Schwartz, G. A.; Jacobsson, P. *Macromolecules* **2002**, *35*, 4337. Janik, P.; Paluch, M.; Ziolo, J.; Sulkowski, W.; Nikiel, L. *Phys. Rev. E* **2001**, *64*, 042502.
(8) Heinrich, G.; Klüppel, M. *Adv. Polym. Sci.* **2002**, *160*, 1.
(9) Klüppel, M. *Adv. Polym. Sci.* **2003**, *164*, 1.
(10) Ward, A. A.; Bishai, A. M.; Hanna, F. F.; Yehia, A. A.; Stoll, B.; von Soden, W.; Herminghaus, S.; Mansour, A. A. *Kaut. Gummi Kuns.* **2006**, 654.

(11) Meier, J. G.; Fritzsche, J.; Guy, L.; Bomal, Y.; Klüppel, M. *Macromolecules* **2009**, *42*, 2127.
(12) Heinrich, G.; Klüppel, M.; Vilgis, T. A. *Curr. Opin. Solid State Mater. Sci.* **2002**, *6*, 195.
(13) Arrighi, V.; McEwen, I. J.; Qian, H.; Serrano Prieto, M. B. *Polymer* **2003**, *44*, 6259.
(14) Schwartz, G. A.; Cerveny, S.; Marzocca, A. J.; Gerspacher, M.; Nikiel, L. *Polymer* **2003**, *44*, 7229.
(15) Robertson, C. G.; Roland, C. M. *Rubber Chem. Technol.* **2008**, *81*, 506.
(16) Kremer, F.; Schönhals, A. *Broadband Dielectric Spectroscopy*; Springer-Verlag: Berlin, 2003.
(17) Schönhals, A.; Goering, H.; Costa, F. R.; Wagenknecht, U.; Heinrich, G. *Macromolecules* **2009**, *42*, 4165.
(18) Asami, K. *Prog. Polym. Sci.* **2002**, *27*, 1617.
(19) Davis, L. C. *J. Appl. Phys.* **1992**, *72*, 1334.
(20) Rica, R. A.; Jiménez, M. L.; Delgado, A. V. *Soft Matter* **2012**, *8*, 3596.
(21) Arous, M.; Ben Arnor, I.; Kallel, A.; Fakhfakh, Z.; Perrier, G. *J. Phys. Chem. Solids* **2007**, *68*, 1405.
(22) Feldman, Y.; Skodvin, T.; Sjoblom, J. Dielectric Properties of Emulsion and Related Colloidal Systems. *Encyclopedic Handbook of Emulsion Technology*: Marcel Dekker: New York, 2000.
(23) Pratt, G. T.; Smith, M. J. A. *Polymer* **1989**, *30*, 1113.
(24) Lee, Y. H.; Bur, A. J.; Roth, S. C.; Start, P. R. *Macromolecules* **2005**, *38*, 3828.
(25) Bohning, M.; Goering, H.; Fritz, A.; Brzezinka, K. W.; Turky, G.; Schönhals, A.; Schartel, B. *Macromolecules* **2005**, *38*, 2764.
(26) Chanmal, C. V.; Jog, J. P. *Express Polym. Lett.* **2008**, *2*, 294.
(27) Meier, J. G.; Mani, J. W.; Klüppel, M. *Phys. Rev. B* **2007**, *75*, 054202.
(28) Carsi, M.; Sanchis, M. J.; Diaz-Calleja, Riande, R. E.; Nugent, M. J. D. *Macromolecules* **2012**, *45*, 3571.
(29) Leyva, M. E.; Barra, G. M. O.; Moreira, A. C. F.; Soares, B. G.; Khastgir, D. *J. Polym. Sci., Part B* **2003**, *41*, 2983.
(30) Mansour, S. A.; Al-ghoury, M. E.; Shalaan, E.; El Eraki, M. H. I.; Abdel-Bary, E. M. *J. Appl. Polym. Sci.* **2011**, *122*, 1226.
(31) Eid, M. A. M.; El-Nashar, D. E. *Polym.-Plast. Technol. Eng.* **2006**, *45*, 675.
(32) Vo, L. T.; Anastasiadis, S. H.; Giannelis, E. P. *Macromolecules* **2011**, *44*, 6162.
(33) Castagna, A. M.; Wang, W.; Winey, K. I.; Runt, J. *Macromolecules* **2011**, *44*, 2791.
(34) Fernández-Berridi, M. J.; González, N.; Mugica, A.; Bernicot, C. *Thermochim. Acta* **2006**, *444*, 65.
(35) Cerveny, S.; Schwartz, G. A.; Otegui, J.; Colmenero, J.; Loichen, J.; Westermann, S. *J. Phys. Chem. C* **2012**, *116*, 24340.
(36) Zhuravlev, L. T. *Colloids Surf., A* **2000**, *173*, 1.
(37) Hanna, F. F.; Bishai, A. M.; Ward, A. A.; Stoll, B.; Göritz, D. *Kaut. Gummi Kuns.* **2004**, *57*, 288.
(38) Nikaj, E.; Stevenson-Royaud, I.; Seytre, G.; David, L.; Espuche, E. *J. Non-Cryst. Solids* **2010**, *356*, 589.
(39) Cole, K. S.; Cole, R. H. *J. Chem. Phys.* **1941**, *9*, 341.
(40) (a) Vogel, H. *Phys. Z.* **1921**, *22*, 645. (b) Fulcher, G. S. *J. Am. Chem. Soc.* **1925**, *8*, 339. Fulcher, G. S. *J. Am. Chem. Soc.* **1925**, *8*, 789.
(41) Banhegyi, G.; Karasz, F. E. *J. Polym. Sci.* **1986**, *24*, 209.
(42) Woo, M.; Piggott, R. *J. Compos.* **1988**, *10*, 16.
(43) Van Beek, L. K. H. *Dielectric Behavior of Heterogeneous Systems*; Progress in Dielectrics Vol. *7*; Heywood Books: London, 1967.
(44) Banhegyi, G. *Colloid Polym. Sci.* **1986**, *264*, 1030.
(45) Dyre, J. C. *J. Phys. C* **1986**, *19*, 5655.
(46) Steeman, P. A. M.; Maurer, F. H. J. *Colloid Polym. Sci.* **1990**, *268*, 315.
(47) Pelster, R. *Phys. Rev. B* **1999**, *59*, 9214.
(48) Steeman, P. A. M.; Maurer, F. H. J.; van ES, M. A. *Polymer* **1991**, *32*, 523.
(49) Datta, S.; Bhattcharya, A. K.; De, S. K.; Kontos, E. G.; Wefer, J. M. *Polymer* **1996**, *37*, 5597.
(50) Fritzsche, J.; Klüppel, M.; Meier, J. G. *Kaut. Gummi Kuns.* **2009**, *62*, 319.
(51) Boucher, V. M.; Cangialosi, D.; Alegría, A.; Colmenero, J.; Gonzalez-Irun, J.; Liz-Marzan, L. M. *Soft Matter* **2010**, *6*, 3306.
(52) Boucher, V. M.; Cangialosi, D.; Alegría, A.; Colmenero, J.; Pastoriza-Santos, I.; Liz-Marzan, L. M. *Soft Matter* **2011**, *7*, 3607.
(53) Cangialosi, D.; Boucher, V. M.; Alegria, A.; Colmenero, J. *Polymer* **2012**, *53*, 1362.
(54) Bogoslovov, R. B.; Roland, C. M.; Ellis, A. R.; Randall, A. M.; Robertson, C. G. *Macromolecules* **2008**, *41*, 1289.
(55) Adam, G.; Gibbs, J. H. *J. Chem. Phys.* **1965**, *43*, 139.
(56) Povolo, F.; Hermida, E. B. *J. Appl. Polym. Sci.* **1995**, *58*, 55.
(57) Povolo, F.; Schwartz, G.; Hermida, E. B. *J. Polym. Sci., Part B: Polym. Phys.* **1996**, *34*, 1257.
(58) Schwartz, G. A.; Cangialosi, D.; Alegría, A.; Colmenero, J. *J. Chem. Phys.* **2006**, *124*, 154904.
(59) Cangialosi, D.; Alegría, A.; Colmenero, J. *Phys. Rev. E* **2007**, *76*, 011514.
(60) Donth, E. *J. Non-Cryst. Solids* **1982**, *53*, 325.
(61) Cerveny, S.; Mattsson, J.; Swenson, J.; Bergman, R. *J. Phys. Chem. B* **2004**, *108*, 11596.